Magnetic anisotropy and superspin glass behavior of Fe nanoparticles embedded in Cr and Ag matrices

D. Peddis[a *], M.T. Qureshi [b,c], S.H. Baker[b], C. Binns[b] , M. Roy[b], S. Laureti[a],

D. Fiorani[a], P. Nordblad[d], R. Mathieu[d],

[a]ISM-CNR, Area della Ricerca, Via salaria Km 29,500, P.B. 10-00016, Monterotondo Scalo, Roma, Italy

[b]Department of Physics and Astronomy, University of Leicester, Leicester LE1 7RH, UK

[c]Department of Physics, Hazara University, Mansehra, Pakistan

[d]Department of Engineering Science, Uppsala University, Box 534, SE-751 21, Uppsala,

Sweden

Abstract

Static and dynamical magnetic properties of Fe nanoparticles (NPs) embedded in non-magnetic (Ag) and antiferromagnetic (Cr) matrices with a volume filling fraction (VFF) of 10% have been investigated. In both Fe@Ag and Fe@Cr nanocomposites, the Fe nanoparticles have a narrow size distribution, with a mean particle diameter around 2 nm. In both samples, the saturation magnetization reaches that of Fe bulk bcc, suggesting the absence of alloying with the matrices. The coercivity at 5 K is much larger in Fe@Cr than in Fe@Ag as a result of the strong interaction between the Fe NPs and the Cr matrix. Temperature-dependent magnetization and ac-susceptibility measurements point out further evidence of the enhanced inter-particle interaction in the Fe@Cr system. While the behavior of Fe@Ag indicates the presence of weakly interacting magnetic monodomain particles with a wide distribution of blocking temperatures, Fe@Cr behaves like a superspin glass produced by the magnetic interaction between nanoparticles.

1. Introduction

Embedding magnetic nano-objects in a magnetic or non-magnetic matrix/shell (nanocomposite [1]) not only allows one to control the morphological and structural properties of a material but is also an effective method to tune interparticle interactions. The nature and strength of magnetic interactions depend on the size and volume fraction of the magnetic nano-entities, and on the structural, textural and magnetic properties of the matrix/shell [2]. In addition, the possibility of modifying the magnetic nature of the matrix enables the introduction of a new source of anisotropy, allowing a further degree of freedom in the design of new materials [3–5]. In particular, the exchange interaction across a ferro (FM) or ferrimagnetic (FI)/antiferromagnetic (AF) interface gives rise to an additional exchange anisotropy, which affects the magnetization reversal process of the whole system, producing significant changes in the coercivity. This phenomenon (exchange bias, EB) consists of a horizontal shift of the hysteresis loop observed when a system with FM (FI)/AF interface is cooled down in a magnetic field through the Néel temperature of the AF material [6,7]. EB was first observed in 1956 in Co/CoO core shell particles [8]; later, relatively few studies in nanoparticle systems were reported [9–11] [12] [13] and most of the research was focused on thin film systems due to their applicability [14–18] [19–22]. Indeed, several advanced magnetic and magnetoelectronic devices rely on interface exchange coupling between different magnetic phases in bilayers and multilayers (e.g.: magnetoresistive recording read heads, magnetoresistive random access memories, spring magnets and magnetic tunnel junctions). In addition, in thin films a better control of the interface microstructure (e.g. grain size, orientation, crystalline quality, roughness, spin structure or interface layer) can be obtained.

In the last fifteen years, the study of EB effects in nanoparticles systems (e.g. core-shell, particles embedded in a matrix) is recovering importance. This is due to the great improvement in the synthesis methods, allowing a better control of the microstructural properties thus opening new perspectives for applications (permanent magnets, magnetic recording, magnetic hyperthermia etc.). Studies of systems consisting of Co particles embedded in an AF manganese matrix have shown that the FM/AF interface exchange coupling also affects the interparticle interactions, leading to spin glass-like dynamics. [23,24]

In this paper we present a magnetic study of ultra-small Fe nanoparticles (~2 nm) embedded at a volume filling fraction (VFF) of 10% in an antiferromagnetic Cr matrix (Fe@Cr) and a non-magnetic Ag matrix (Fe@Ag). A comparison between the two systems highlights the influence of the FM/AF interface exchange coupling on the reversal mechanisms of magnetization as well as on the magnetization dynamics.

2. Experimental

Fe@Cr and Fe@Ag nanocomposites were prepared in the form of films (~200 nm thickness) by co-depositing Fe nanoparticles and the Cr and Ag matrix respectively, using a gas aggregation cluster source and a molecular beam epitaxy (MBE) source on poly-ether-ether-ketone (PEEK) substrates. A buffer and a capping layer of Ag was deposited (from an MBE source) in order to protect the films against oxidation after removal from the deposition chamber [25]. The deposition rates of the Fe particles and Cr or Ag matrix materials at the substrate were measured by means of a quartz crystal thickness monitor. Using these data, the volume filling fraction (VFF) of the particles within the film, i.e. the ratio between the equivalent thickness of the deposited particles and the total thickness of the film, is derived. By appropriately choosing the deposition rates samples with Fe 10% VFF have been prepared. The cluster source produces a log-normal distribution of cluster sizes, as measured in situ by an axially mounted quadrupole filter (Fig.1). Particle size diameter has been well fitted by a log normal function (continuous lines):

$$P(D) = \frac{100}{D\,\sigma\,\sqrt{2\pi}} \exp - \left(\ln^2 \frac{(D / < D_{TEM} >)}{2\sigma^2} \right) \qquad (1)$$

where $<D_{TEM}>$ is the median of the variable "diameter", often used to estimate the average diameter of nanoparticles [26–28] and σ, the standard deviation of the natural logarithm of the variable D. The log-normal fits indicate a mean particle diameter of 2.0 ± 0.1 nm and 2.1 ± 0.1 nm for Fe@Cr and Fe@Ag,

respectively. On the other hand, the particle size distribution appears to be larger for the Fe@Ag sample, with a σ value 0.25 compared to 0.14 for Fe@Cr. For reference, a third sample composed of only the Cr matrix was synthesized under the same conditions.

Magnetic measurements were carried out using a SQUID magnetometer. The magnetization M vs. T was measured in zero field cooled (ZFC) and field cooled (FC) conditions: the samples were cooled from 300 K down to 5 K in zero magnetic field; then a static magnetic field $H_{.}$ was applied and the magnetization M_{ZFC} was measured on warming up to 300 K; finally the sample was cooled down to 5 K under the same H-field while measuring the magnetization M_{FC}. M vs H measurements, were performed at 5 K after either ZFC or FC ($\mu_0 H_{cool.}$= 1T) from 300 K. The ac-susceptibility $\chi(T,f)$ was recorded as a function of temperature for different frequencies, f, of the ac-excitation of amplitude h = 0.4 mT. $\chi(T,f)$ curves were also recorded under applied dc bias magnetic fields.

3 Results and Discussion

Recent detailed structural investigations using Extended X-ray Absorption Fine Structure (EXAFS) have been carried out on Fe@Cr nanocomposites with VFFs in the range 5-20 % [9]. These studies showed that the atomic structure of the Cr-embedded Fe nanoparticles is the same as the bulk bcc structure. Whereas alloying between the nanoparticles and the matrix material has been previously shown to be very pronounced for Co nanoparticles in antiferromagnetic Mn[2], it was found that alloying between Fe nanoparticles and Cr matrix material is limited [10]. Previous studies on Fe@Ag showed that also in this case Fe retains the bcc structure and no alloying is observed [29,30]. This is confirmed by the saturation magnetization (M_S) values obtained by analyzing the ZFC hysteresis loops recorded at T = 5 K (figure 2a). M_S values close to that of the bulk bcc Fe (1714 kA/m) were obtained for both Fe@Cr and Fe@Ag nanocomposites. An M vs. H curve for the pure Cr matrix was also recorded at 5 K (figure 2a and detail in figure S1) and despite the antiferromagnetic nature of Cr, it shows a weak ferromagnetism (~ 20 kA/m), associated with uncompensated magnetic moments, as also observed for a Mn matrix produced with the same synthesis method [31].

On the other hand, the ZFC hysteresis loops of the Fe@Cr and Fe@Ag samples are quite different at lower magnetic fields: taking the irreversibility field as the splitting point between the magnetizing and demagnetizing branches of the M vs H curve (the field where the difference, normalized to the M_S value, becomes ≈ 1%) the saturation field $\mu_0 H_K$ was estimated. $\mu_0 H_K$ can be considered as the maximum applied field required to reverse the magnetisation of the particle with the highest anisotropy energy. $\mu_0 H_K$ is significantly lower in Fe@Ag ($\mu_0 H_K \approx 0.2$ T) compared to Fe@Cr ($\mu_0 H_K \approx 2$ T). This suggests the presence of exchange interactions between the Fe particles and the Cr matrix, hindering the reversal of magnetization and increasing the magnetic anisotropy of the whole system [32]. Considering the relation $K_{eff} = \mu_0 H_K M_s/2$ [28,33], we could estimate for Fe@Ag an effective anisotropy constant K_{eff} of the order of 1.7×10^5 J/m^3 at 5K, which is only slightly larger than the bulk value in agreement with earlier studies[3]. In the Fe@Cr sample, being H_K 10 times larger than in Fe@Ag, the Fe/AF exchange interaction results in a much larger affective anisotropy (K_{eff} Fe@Cr : 1.7×10^6 J/m^3).

The effect of the particle/matrix exchange interaction is also evident in the hysteresis curves recorded after FC under 1T, as shown in Fig. 2b. In the case of Fe@Ag, the ZFC and FC hysteresis curves overlap with a coercive field $\mu_0 H_c \approx 18$ mT, indicating lack of exchange bias in the system. On the other hand, a small, but significant exchange bias is observed in the Fe@Cr nanocomposite, as the FC curves are horizontally shifted toward negative magnetic fields. The exchange bias field ($\mu_0 H_{EB} = -(H_{c+} + H_{c-})/2$) is about 5 mT at 5 K, while the field-cooled coercivity H_{cFC} amounts to 45 mT, i.e. slightly larger than the ZFC one ($\mu_0 H_{cZFC} \sim 40$ mT). The exchange bias and increase of coercivity are other indications of the magnetic interaction of the Fe nanoparticles with the Cr matrix and increased anisotropy in the system. Here the H_{EB}/H_{cFC} ratio is about 0.1, while it is larger than 0.3 in the above mentioned Co@Mn system ($\mu_0 H_{EB} \sim 75$

mT, $\mu_0 H_{cFC}$ ~ 220 mT) [35]; note that VFF (5%) was different in that case. It has been shown in the Fe@Cr system that the H_{EB}/Hc_{FC} ratio is only 0.05 for a VFF of 5%, with maximum value close to 0.2 for a VFF of 20% [10].

The effect of the Cr/Ag matrix is also evident in temperature dependent magnetization measurements. Fig. 3 shows the ZFC/FC curves recorded in a small magnetic field ($\mu_0 H$ = 1 mT) for Fe@Ag and Fe@Cr. The ZFC/FC curves of the Fe@Ag are typical of a system of weakly interacting nanoparticles, with a broad maximum around 150 K in the ZFC magnetization, and a deviation from the Curie-like behaviour in FC curve at lower temperatures. A K_{eff} value of 1.7×10^5 J/m^3 was extracted above from the M(H) curves depicted in Fig.2. If the dynamics would follow an Arrhenius-type behavior reflecting the lack of interparticle interaction, this K_{eff} would imply, considering the volume V (from diameter d ~ 2 nm) and the relation $K_{eff}V \sim 25\ k_B T_b$ (k_B is the Boltzmann constant) [36], a blocking temperature T_b of the order of 10 K.

In order to evaluate T_b the low field M_{FC-ZFC} magnetization curve (inset figure 3a) has been investigated. For non-interacting particles, the derivative of this curve gives an estimate of the anisotropy energy barrier distribution:

$$f(\Delta E_a) \propto -\frac{dM_{FC-ZFC}}{dT} \qquad (2)$$

Because of the presence of weak interparticle interactions in our samples, the derivative of M_{FC-ZFC} (inset figure 3a) can actually be considered only as estimation of the E_a distribution, including the effect of the interparticle interactions themselves. Within the Néel model, the blocking temperature can be defined as the temperature for which the relaxation time is equal to the measuring time of the experimental technique. In a real system of nanoparticles, where a finite size distribution always exist, T_b is often defined as the temperature at which 50% of the sample is in the superparamagnetic state [37]. Since T_b is proportional to E_a, an estimate of the T_b distribution can be obtained from the E_a distribution by evaluating the temperature at which 50% of the particles overcome their anisotropy energy barriers. For Fe@Ag sample a blocking temperature of 70 K has been found a maximum that is much broader than expected from the relative sharp particle size distribution. The increase of blocking temperature can partly be ascribed to the presence of dipolar and some RKKY-like interparticle interactions. However, the very broad maximum and the unexpectedly high blocking temperature also indicate a broad distribution of anisotropy energy shifted towards higher energy than indicated by the particle size. This could be ascribed to some clustering phenomena, yielding an inhomogeneous distribution of particles within the matrix (i.e. wide distribution of interparticle distance). That effect has been already well discussed in Fe@Ag systems prepared by gas phase synthesis [38], showing that for volume filling fraction of 10% some clustering is observed. Only for VFF below 1-2 % the clustering process can be avoided. Such behaviour has been also observed in other nanoparticle systems [37,39].

The ZFC curves of the Fe@Cr nanocomposite exhibit instead a sharper maximum near 150 K. While the FC curve closely follows the ZFC one from high temperature down to the maximum temperature, the FC magnetization completely flattens, after exhibiting a broad maximum near 100 K. The cusp-like in ZFC magnetization and flat FC magnetization is similar to those observed in spin and superspin glasses [40] [41,42]. In nanoparticle systems, the glassy behaviour results from the random magnetic interaction and frustration between particles or superspins [43]. The results thus suggests that the Cr matrix mediates a stronger magnetic interaction between the Fe nanoparticles than the non-magnetic, Ag one. Similar effects have been reported in the Co@Ag / Co@Mn systems: Co@Ag was found to display superparamagnetic properties while a spin-glass-like behaviour were observed in Co@Mn with the same VFF [24,44]. Fig. S2 in the s.m. shows ZFC/FC curves of the Fe@Cr systems with 5% VFF, 10% VFF and 20% VFF (c.f. Ref. [10]). While the VFF 5% nanocomposite displays presence of weakly interacting nanoparticles with weak (but significant) interaction, the 20% VFF nanocomposite behaves as a ferromagnet [45]. A similar magnetic state was observed in Fe@Mn 24.8 % VVF [10] suggesting that 20%

represents the percolation threshold where significant clustering of nanoparticles occurs.

The temperature dependence of the in-phase component of the ac-susceptibility $\chi'(T, f)$ and out-of-phase component $\chi''(T,f)$ is presented in figure 4 for Fe@Ag and Fe@Cr. Both $\chi'(T,f)$ and $\chi''(T,f)$ of Fe@Ag exhibit broad peaks [5,46]. On the other hand in Fe@Cr, $\chi'(T,f)$ displays quite sharp maxima, and $\chi''(T,f)$ increases rapidly as the temperature is decreased from 300 K, as observed at a (super)spin glass phase transition [47]. The susceptibility is frequency dependent near the cusp temperatures, which we denote the freezing temperatures $T_f(f)$. The frequency dependence of $\chi'(T,f)$ decreases as the temperature is further lowered, and accordingly $\chi''(T,f)$ rapidly decreases with decreasing temperature as observed in glassy systems composed of superspins rather than single, atomic spins [47,48]. The ac-susceptibility curves of Fe@Cr were also measured under a superimposed dc magnetic field (see Fig. 4). It can be seen that a relatively small bias field of 1 mT significantly affects the susceptibility curves. Under a bias field of 10 mT, the susceptibility curves are further suppressed, leaving only the low-temperature susceptibility unaffected.

The glassy behaviour of the system can be further evidenced by performing so called memory experiments [49], collected on heating the ZFC magnetization as a function of temperature after including halts at a specific temperature (T_h) in the cooling. In spin glasses and superspin glasses cooled down to T_h, below the glass phase transition temperature T_g, the spin or superspin configuration will be out of equilibrium and will slowly rearrange itself toward the equilibrium state at T_h [47,49]. If the system is further cooled to the lowest temperature available, this equilibration, or aging, will be kept in memory and retrieved on reheating. The ZFC magnetization recorded after a given wait time at constant temperature T_h during cooling is lower around this temperature than if the magnetization is recorded without the halt. Thus the memory of the equilibrations will appear as "memory dips" [49] in the magnetization curves. These dips are blown-up in difference plots of ZFC magnetization curves recorded with and without halts at T_h. The main frame of Fig. 5 shows ZFC reference and memory curves with halts at 50 or 85 K. The inset of Fig. 5 shows the corresponding difference plots. Halts of different duration were used at 50 K and the memory dips are more pronounced if equilibration has been allowed to proceed for a longer time. These results indicate that spin glass like aging, memory and rejuvenation [49,50] phenomena occur in Fe@Cr. Interestingly, no memory effect was observed in the Fe@Ag nanocomposite which indicates that collective interaction phenomena are absent and that the unexpectedly high blocking temperature and broad ZFC maxima are to be assigned to individual particle and clustered particle relaxation.

4 Conclusion

We have investigated two nanocomposites consisting of Fe nanoparticles with a narrow size distribution around 2 nm dispersed in metallic non-magnetic (Ag) or antiferromagnetic (Cr) matrices with volume filling fraction of 10 %. The anisotropy and the magnetization reversal process of the particles in Fe@Cr are greatly affected by the Fe/Cr interface exchange coupling. The Fe@Cr system was found to behave as a superspin glass.

Acknowledgements

Financial support from the Swedish Research Council (VR) and the Göran Gustafsson Foundation is acknowledged. D. Peddis gratefully acknowledges the COST action MP1308 "Towards Oxide based electronics" for the support of its research activity at the Uppsala University (STSM program).

Bibliography

[1] S. Komarneni, 2 (1992) p.1219.

[2] C. Caizer, Phys. B Condens. Matter 327 (2003) p.27.

[3] D. Peddis, S. Laureti, M. V. V Mansilla, E. Agostinelli, G. Varvaro, C. Cannas, and D. Fiorani, Superlattices Microstruct. 46 (2009) p.125.

[4] V. Skumryev, S. Stoyanov, Y. Zhang, G. Hadjipanayis, D. Givord, and J. Nogues, Nature 423 (2003) p.850.

[5] D. Peddis, P. E. Jonsson, G. Varvaro, and S. Laureti, in *Nanomagnetism Fundam. Appl.*, edited by C. Binns (Elsevier B.V, Oxford, UK, 2014).

[6] J. Nogués and I. K. Schuller, J. Magn. Magn. Mater. 192 (1999) p.203.

[7] F. Nolting, a Scholl, J. Stohr, J. Seo, J. Fompeyrine, H. Siegwart, J. Locquet, S. Anders, J. Luning, E. Fullerton, M. Toney, M. Scheinfein, and H. Padmore, Nature 405 (2000) p.767.

[8] W. H. Meiklejohn and C. P. Bean, Phys. Rev. 102 (1956) p.1413.

[9] S. Laureti, D. Peddis, L. Del Bianco, A. M. Testa, G. Varvaro, E. Agostinelli, C. Binns, and S. Baker, J. Magn. Magn. Mater. 324 (2012) p.3503.

[10] M. T. Qureshi, S. H. Baker, C. Binns, M. Roy, S. Laureti, D. Fiorani, and D. Peddis, J. Magn. Magn. Mater. 378 (2015) p.345.

[11] C. Binns, M. T. Qureshi, D. Peddis, S. H. Baker, P. B. Howes, A. Boatwright, S. A. Cavill, S. S. Dhesi, L. Lari, R. Kroger, and S. Langridge, Nanoletters 13 (2013) p.3334.

[12] P. J. van der Zaag, Y. Ijiri, J. a Borchers, L. F. Feiner, R. M. Wolf, J. M. Gaines, R. W. Erwin, and M. a Verheijen, Phys. Rev. Lett. 84 (2000) p.6102.

[13] M. Estrader, a López-Ortega, S. Estradé, I. V Golosovsky, G. Salazar-Alvarez, M. Vasilakaki, K. N. Trohidou, M. Varela, D. C. Stanley, M. Sinko, M. J. Pechan, D. J. Keavney, F. Peiró, S. Suriñach, M. D. Baró, and J. Nogués, Nat. Commun. 4 (2013) p.2960.

[14] S. Laureti, L. Del Bianco, B. Detlefs, E. Agostinelli, V. Foglietti, D. Peddis, a. M. Testa, G. Varvaro, and D. Fiorani, Thin Solid Films 543 (2013) p.162.

[15] S. Laureti, S. Y. Suck, H. Haas, E. Prestat, O. Bourgeois, and D. Givord, Phys. Rev. Lett. 108 (2012) p.77205.

[16] K. O. Grady, K. O'Grady, L. E. E. Fernandez-Outon, G. Vallejo-Fernandez, and K. O'Grady, J. Magn. Magn. Mater. 322 (2010) p.883.

[17] M. Kovylina, M. G. del Muro, Z. Konstantinović, M. Varela, O. Iglesias, A. Labarta, and X. Batlle, Nanotechnology 20 (2009) p.175702.

[18] J. Nogués, J. Sort, V. Langlais, V. Skumryev, S. Suriñach, J. S. Muñoz, and M. D. Baró, Phys. Rep. 422 (2005) p.65.

[19] F. Parker, K. Takano, and a. Berkowitz, Phys. Rev. B 61 (2000) p.R866.

[20] S. Brück, J. Sort, V. Baltz, S. Suriñach, J. S. Muñoz, B. Dieny, M. D. Baró, and J. Nogués, Adv. Mater. 17 (2005) p.2978.

[21] M. Ali, P. Adie, C. H. Marrows, D. Greig, B. J. Hickey, and R. L. Stamps, Nat. Mater. 6 (2007) p.70.

[22] M. Stiles and R. McMichael, Phys. Rev. B 60 (1999) p.12950.

[23] D. Fiorani, L. Del Bianco, a. Testa, and K. Trohidou, Phys. Rev. B 73 (2006) p.092403.

[24] N. Domingo, D. Fiorani, A. M. Testa, C. Binns, S. Baker, and J. Tejada, J. Phys. D. Appl. Phys. 41 (2008) p.134009.

[25] S. H. Baker, S. C. Thornton, K. W. Edmonds, M. J. Maher, C. Norris, and C. Binns, Rev. Sci. Instrum. 71 (2000) p.3178.

[26] L. B. Kiss, J. Soderlund, G. A. Niklasson, and C. G. Granqvist, Nanotechnlogy 19 (1999) p.25.

[27] A. T. Ngo, P. Bonville, and M. P. Pileni, Eur. Phys. J. B 592 (1999) p.583.

[28] G. Muscas, G. Singh, W. R. Glomm, R. Mathieu, P. A. Kumar, G. Concas, E. Agostinelli, and D. Peddis, Chem. Mater. 27 (2015) p.1982.

[29] C. Binns, M. J. Maher, Q. A. Pankhurst, D. Kechrakos, and K. N. Trohidou, Phys. Rev. B 66 (2002) p.184413.

[30] C. Binns and M. J. Maher, New J. Phys. 4 (2002) p.85.

[31] C. Binns, N. Domingo, A. M. Testa, D. Fiorani, K. N. Trohidou, M. Vasilakaki, J. a Blackman, A. M. Asaduzzaman, S. Baker, M. Roy, D. Peddis, and J. A. Balckman, J. Phys. Condens. Matter 22 (2010) p.436005.

[32] L. Del Bianco, A. Hernando, M. Multigner, C. Prados, J. C. Sanchez-Lopez, A. Fernandez, C. F. Conde, and A. Conde, J. Appl. Phys. 84 (1998) p.2189.

[33] R. H. Kodama, A. E. Berkowitz, E. McNiff, S. Foner, and J. E. J. McNiff, Phys. Rev. Lett. 77 (1996) p.394.

[34] L. Del Bianco, A. Hernando, M. Multigner, C. Pradoc, J. C. Sanchez-Lopez, A. Fernandez, C. F. Conde, and A. Conde, J. Appl. Phys. (1998).

[35] N. Domingo, A. M. Testa, D. Fiorani, C. Binns, S. Baker, and J. Tejada, J. Magn. Magn. Mater. 316 (2007) p.155.

[36] D. L. Leslie-Pelecky and R. D. Rieke, Chemstry Mater. 8 (1996) p.1770.

[37] D. Peddis, C. Cannas, A. Musinu, A. Ardu, F. Orru, D. Fiorani, S. Laureti, D. Rinaldi, G. Muscas, G. Concas, and G. Piccaluga, Chem. Mater. 25 (2013) p.2005.

[38] C. Binns, K. N. Trohidou, J. Bansmann, S. H. Baker, J. a Blackman, J.-P. Bucher, D. Kechrakos, a Kleibert, S. Louch, K.-H. Meiwes-Broer, G. M. Pastor, a Perez, and Y. Xie, J. Phys. D. Appl. Phys. 38 (2005) p.R357.

[39] M. P. Pileni, J. Phys. D. Appl. Phys. 41 (2008) p.134002.

[40] M. S. Andersson, J. A. De Toro, S. S. Lee, R. Mathieu, and P. Nordblad, EPL (Europhysics Lett. 108 (2014) p.17004.

[41] D. Parker, V. Dupuis, F. Ladieu, J. P. Bouchaud, E. Dubois, R. Perzynski, and E. Vincent, Phys. Rev. B 77 (2008) p.104428.

[42] D. Peddis, M. Vasilakaki, K. N. Trohidou, D. Fiorani, N. Ricerche, and A. M. Measurements, IEEE Trans. Magn. 50 (2014) p.6.

[43] P.E. JÖnsson, Adv. Chem. Phys. 128 (2004) p.191.

[44] M. Vasilakaki, K. N. Trohidou, D. Peddis, D. Fiorani, R. Mathieu, M. Hudl, P. Nordblad, C. Binns, and S. Baker, Phys. Rev. B 140402 (2013) p.1.

[45] S. Bedanta and W. Kleemann, J. Phys. D. Appl. Phys. 42 (2009) p.013001.

[46] P. E. Jönsson, R. Mathieu, P. Nordblad, H. Yoshino, H. A. Katori, and A. Ito, Phys. Rev. B 70 (2004) p.174402.

[47] P. A. Kumar, G. Singh, W. R. Glomm, D. Peddis, E. Wahlström, and R. Mathieu, Mater. Res. Express 1 (2014) p.036103.

[48] P. A. Kumar, R. Mathieu, P. Nordblad, S. Ray, O. Karis, G. Andersson, and D. D. Sarma, Phys. Rev. X 011037 (2014) p.12.

[49] D. N. H. Nam, P. Nordblad, R. Mathieu, and P. Jönsson, Phys. Rev. B 63 (2001) p.92401.

[50] R. Mathieu, P. E. Jönsson, P. Nordblad, H. A. Katori, and A. Ito, Phys. Rev. B 65 (2001) p.4.

Figures & Captions

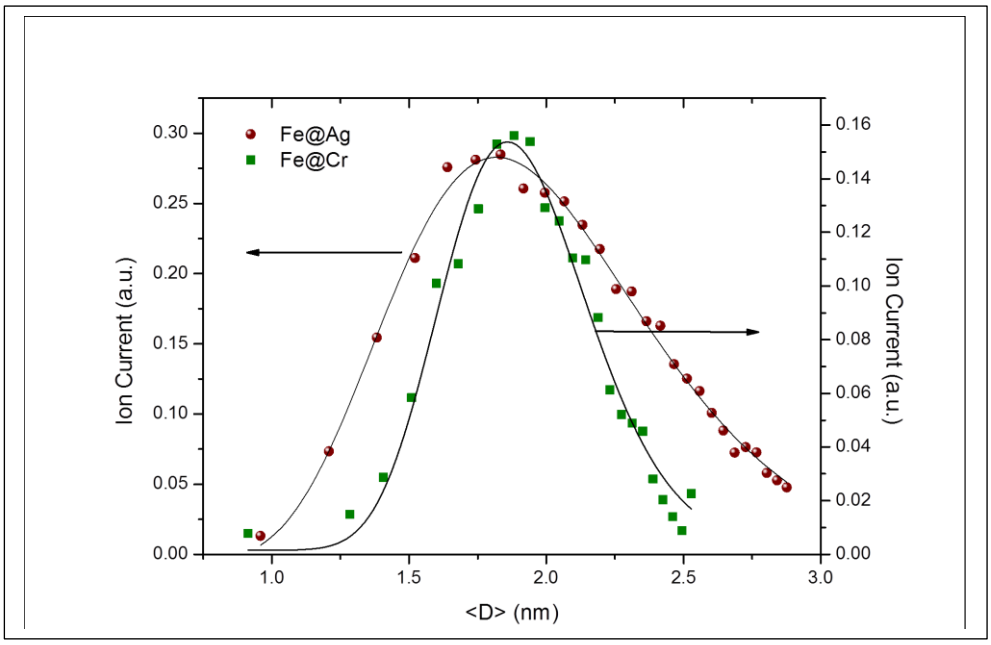

Figure 1: Mass spectrum of gas phase Fe nanoparticles co-deposited with Ag (full circles) and with Cr (full squares).

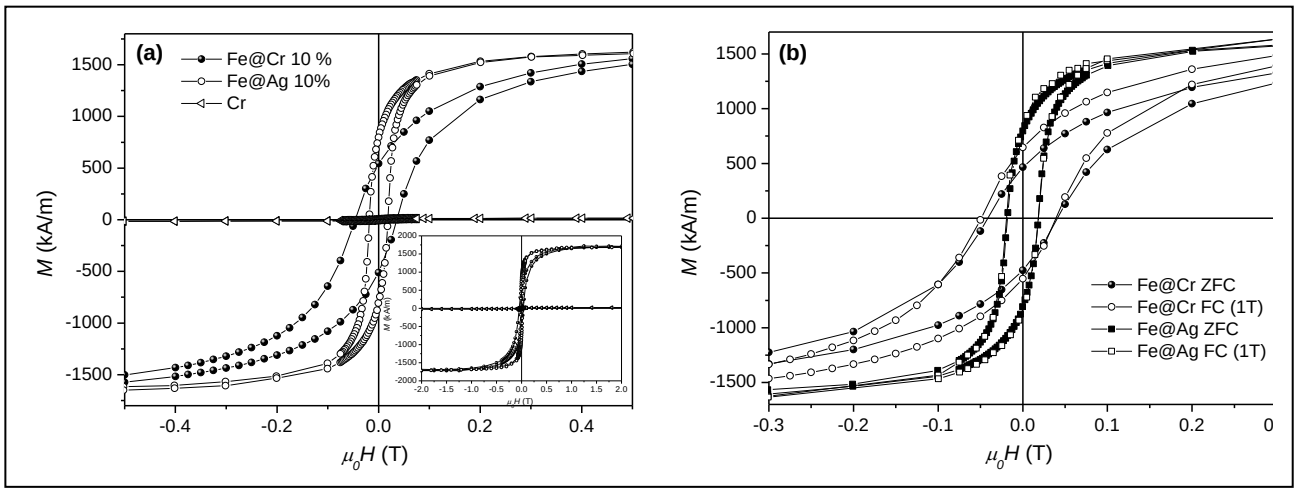

Figure 2: (a): Hysteresis loop recorded at 5K in the field range ±0.5 T measured after ZFC for Fe@Cr (full circles), Fe@Ag (empty circles), Cr (empty triangles) samples. The inset shows loops on the ±2T; (b) ZFC (full symbols) and FC (empty symbols) magnetization recorded under an applied field of 1 T at 5 K for the samples Fe@Cr (circles) and Fe@Ag (squares)

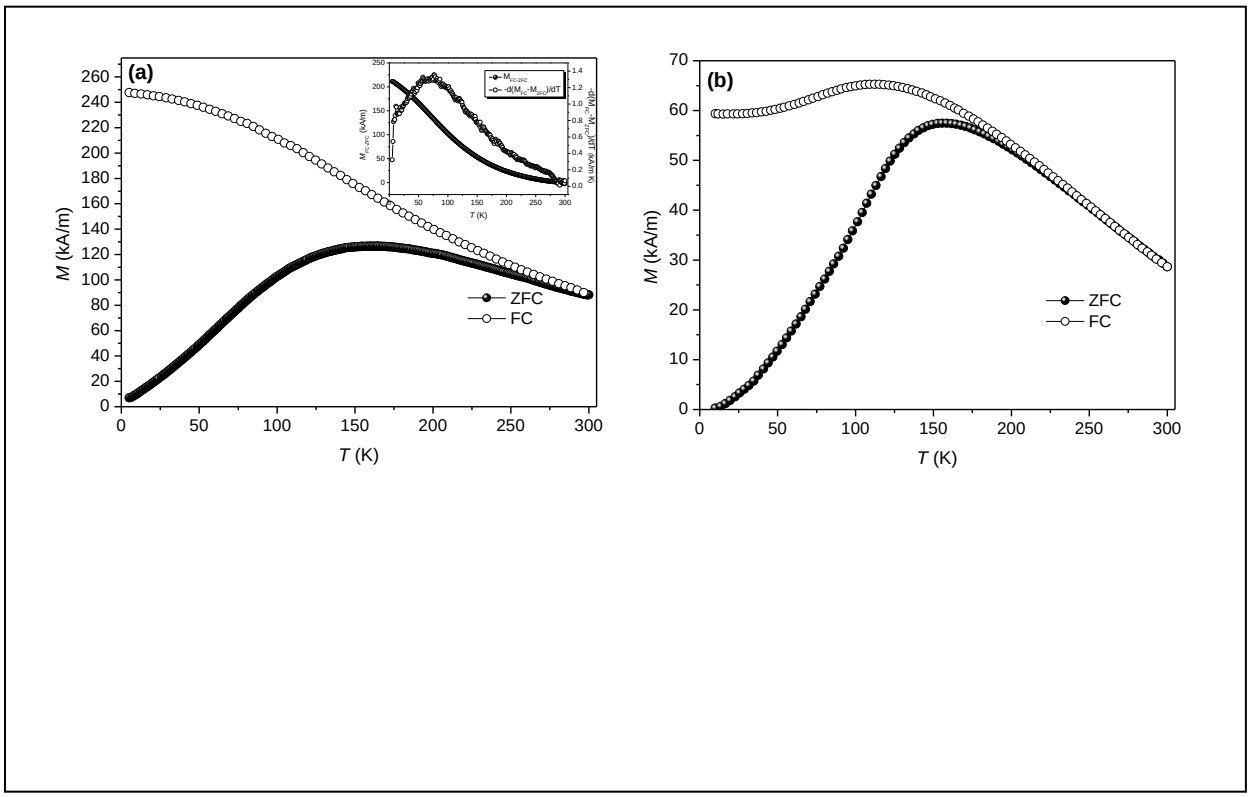

Figure 3: ZFC and FC magnetization curves recorded with an applied field of 1 mT for Fe@Ag (a), Fe@Cr (b) samples; inset fig. 3a difference between field-cooled and zero-field-cooled magnetizations (MFC-MZFC, filled symbols) for Fe@Ag and its temperature derivative ($d(M_{FC}-M_{ZFC})/dT$), open symbols); $\mu_0 H$=1 mT.

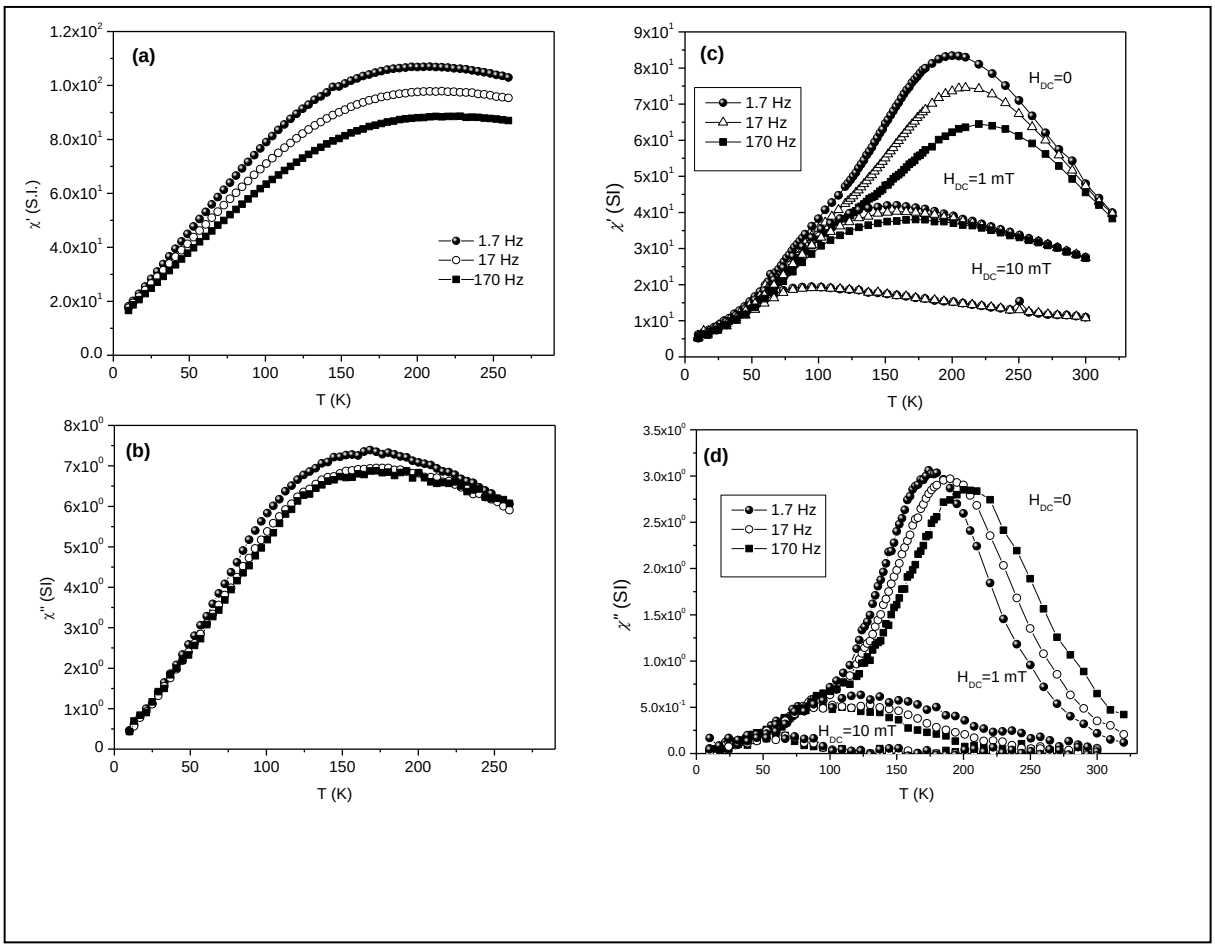

Figure 4: *In-phase*, χ', and (b) *out-of-phase* ,χ'', components of the ac-susceptibility for (a-b) Fe@Ag and (c-d) Fe@Cr nanocomposites; in Fe@Cr case, in-phase and out-of phase components were also recorded in dc bias magnetic fields of 1mT and 10 mT.

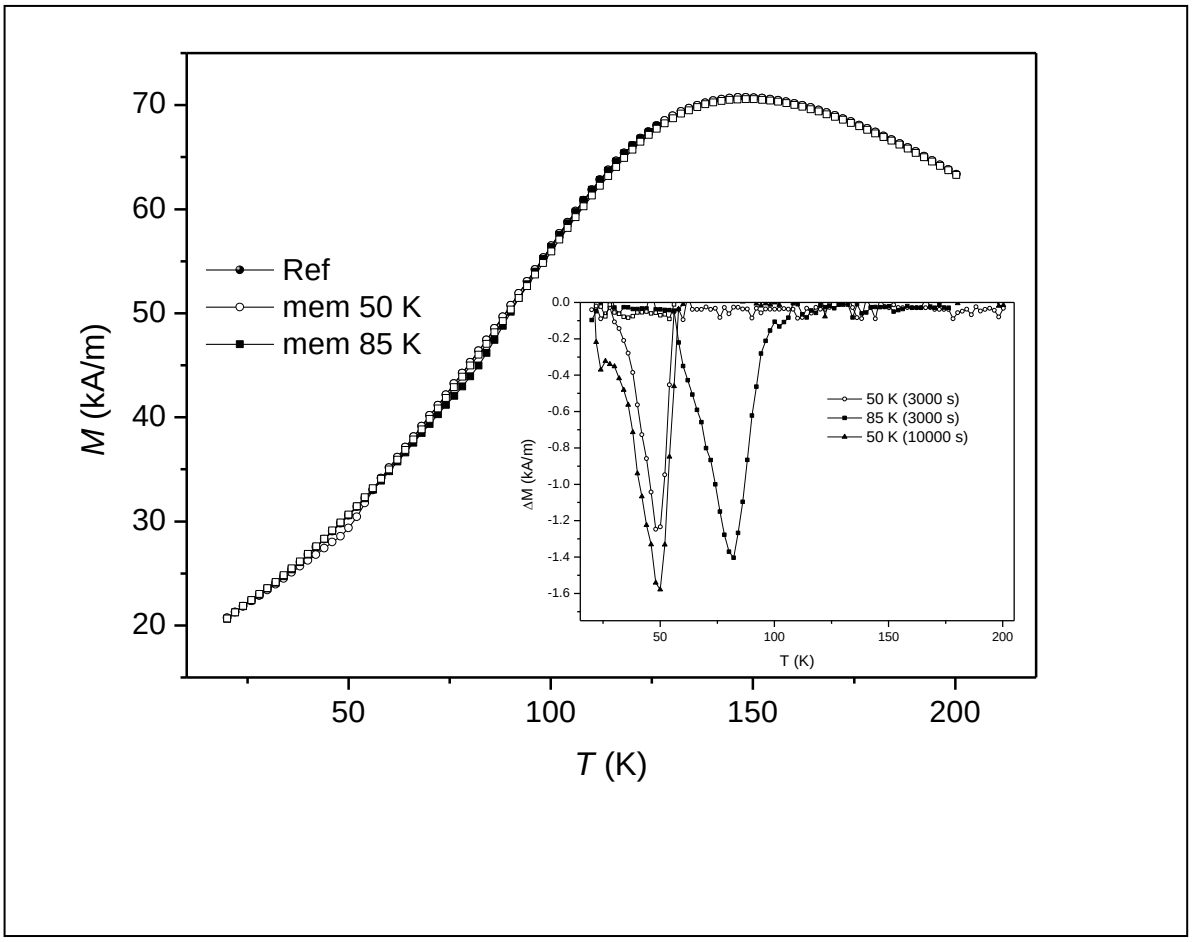

Figure 5: Main frame: ZFC magnetization recorded in an applied field of 1mT after direct cooling to 20 K (full circles) and including halts of 3000 s (empty squares) and 10000 s (full tringles) at 50 K and 85 K (full squares) before reaching 20 K: inset difference between ZFC curves recorded with and without halts in the cooling.

Supporting Information

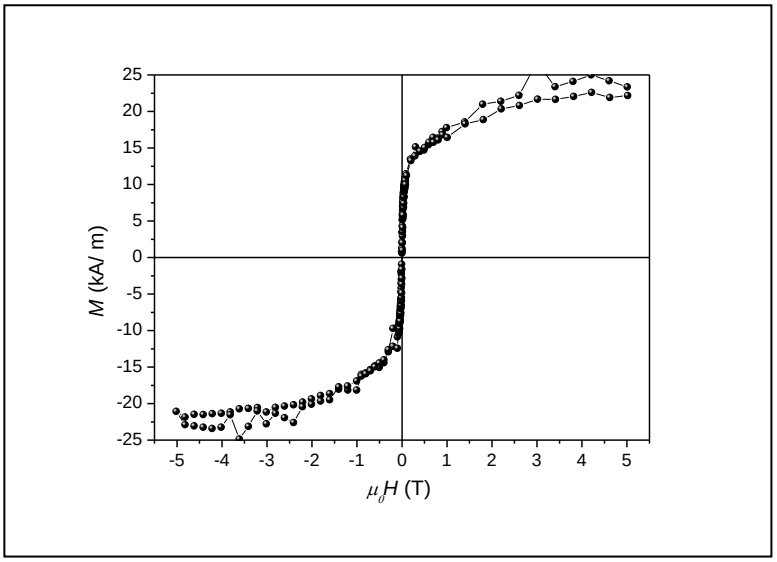

Figure S1: Field dependence of Magnetization of Cr matrix recorded at 5K.

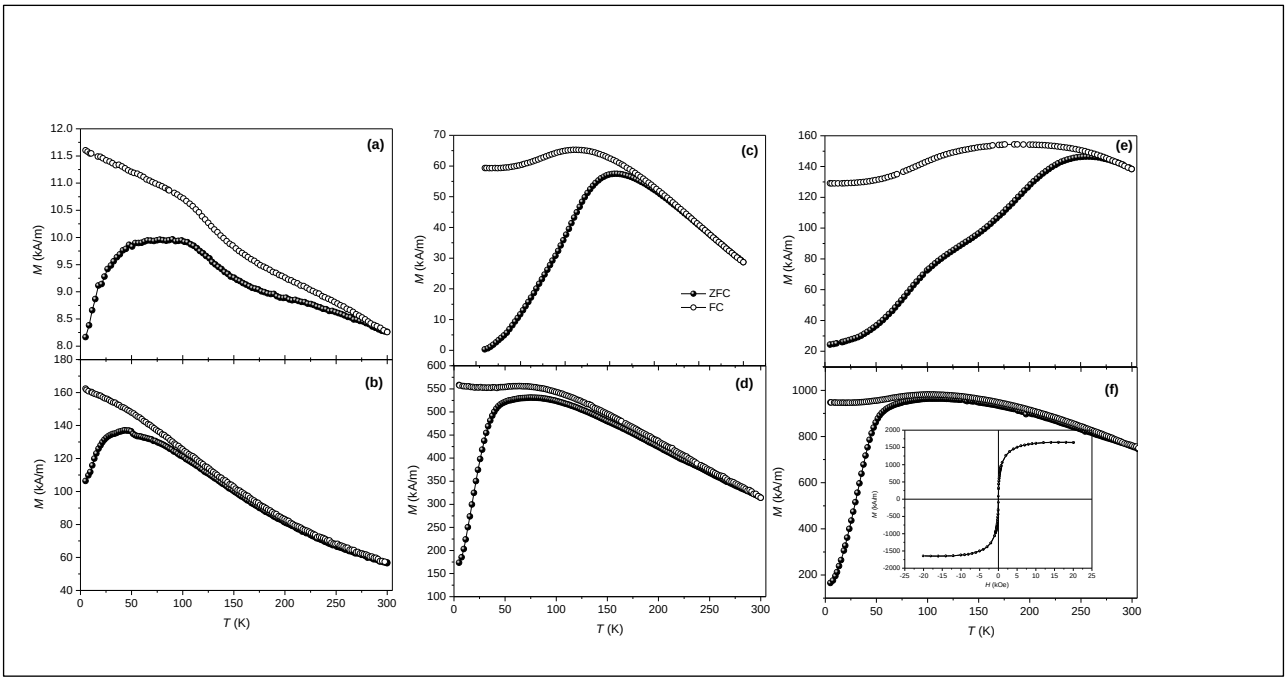

Figure S2: ZFC (full symbols) and FC (empty symbols) magnetization recorded under an applied field of 1 mT (upper panels) and 30 mT (lower panels) for the samples Fe@Cr with VFF= 5 %(a,b), 10 % (c,d), and 20 % (e,f). Inset shows magnetic hysteresis loop recorded at 300 K.